The dielectric behaviour of doped near-stoichiometric lithium niobate in the terahertz range*

Wu Liang(吴 亮)[a], Ling Fu-Ri(凌福日)[a)†], Zuo Zhi-Gao(左志高)[a)], Liu Jin-Song(刘劲松)[a)], and Yao Jian-Quan(姚建铨)[a)b)]

[a)] *Wuhan National Laboratory for Optoelectronics, School of Optoelectronic Science and Engineering, Huazhong University of Science and Technology, Wuhan* 430074, *China*

[b)] *College of Precision Instrument and Optoelectronics Engineering, Tianjin University, Tianjin* 300072, *China*

(Received 30 June 2011; revised manuscript received 4 September 2011)

The dielectric properties of near-stoichiometric $LiNbO_3$:Fe and $LiNbO_3$:Ce single crystals have been investigated using terahertz time domain spectroscopy in a frequency range of 0.7–1.6 THz at room temperature. When coupled with an applied external optical field, obvious photorefractive effects were observed, resulting in a modulation of the complex dielectric constant for the crystals. The variation in refractive index, $|\Delta n|$, had a linear relationship with the applied light intensity, accompanied by a step-like decrease at high intensity. The findings were attributed to the internal space charge field of the photorefraction and the light-induced domain reversal in the crystals.

Keywords: near-stoichiometric $LiNbO_3$, terahertz, photorefraction, domain reversal

PACS: 78.20.Mg, 42.70.Mp, 87.50.U– **DOI:** 10.1088/1674-1056/21/1/017802

1. Introduction

The ferroelectric lithium niobate ($LiNbO_3$, abbreviated as LN) crystal is one of the most widely used materials because of its remarkable electro-optical, acousto-optical, ferroelectric and nonlinear optical properties.[1] The LN is extensively exploited in various applications, such as holographic volume storage, optical image and signal processing, phase conjugation, real-time interferometry, beam deflection, and novelty filters. It is also a typical polar material that exhibits a large pyroelectric effect. The periodically poled $LiNbO_3$ (PPLN) has been widely investigated as an important nonlinear optical waveguide.[2−8] Kajmann *et al.*[9] proposed a light-induced poling inversal method in 1994, which has been developed in recent years to be a promising method for domain engineering. Wang *et al.*[10] reported that the coercive field of differently doped LN crystals could be reduced in the illuminated area, which is important for the light pattern to be transferred into a domain pattern with a homogeneous electric field.

The photorefractive properties of $LiNbO_3$ crystals have been optimized by doping with transition-metal impurities, especially iron in the past. A lot of work has been carried out to investigate the transport processes in the crystal at the usual continuous wave laser intensities (> 100 mW/cm^2), which are now well understood.[1,11−14] However, additional effects could also be observed in the crystal at high light intensities, which cannot be described by the conventional model. For practical applications, it is necessary for the permittivity to be modulated over as wide a range as possible around room temperature. In this paper, we report the terahertz (THz) spectroscopy of near-stoichiometric LN:Fe and LN:Ce single crystals, as well as the variation in their dielectric properties under an external optical field. A light-induced domain reversal in the crystals is also observed in the measurement.

2. Experiment

A near-stoichiometric $LiNbO_3$:Fe (near-SLN:Fe) crystal and a near-stoichiometric $LiNbO_3$:Ce (near-SLN:Ce) crystal were grown using the Czochralski and

*Project supported by the National Natural Science Foundation of China (Grant No. 10974063), the Research Foundation of Wuhan National Laboratory, China (Grant No. P080008), and the National Basic Research Program of China (Grant No. 2007CB310403).

†Corresponding author. E-mail: lingfuri@163.com

© 2012 Chinese Physical Society and IOP Publishing Ltd

TSSG (top-seeded-solution-growth) techniques, which contained 0.1 wt.% of Fe and 0.2 wt.% of Ce, respectively. The ratio of Li to Nb, which was estimated from the Curie temperature measurement, was higher than 49.8/50.2. The crystals were cut and polished to form plates with polar faces perpendicular to the z axis, and dimensions of 10 ×10 ×0.125 mm and 10 ×10 ×0.15 mm.

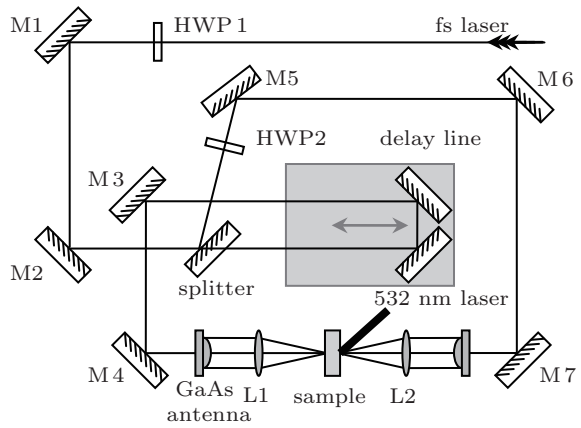


Fig. 1. An installation diagram of time domain spectroscopy. A green laser was obliquely incident on the surface of the sample at an angle of 45° with the polar axis.

We used a terahertz time domain spectroscopy (THz-TDS)[15−17] system to measure the transmission spectra and the dielectric constants of the samples at room temperature, as shown in Fig. 1. In the THz-TDS system, a model-locked Ti:sapphire femtosecond laser beam (centre wavelength 800 nm, repetition rate 80 MHz) was divided into two beams via a beam splitter. The pump beam propagated through a delay line, and was then focused on a GaAs photoconductive antenna under a 20 V direct-current bias for the generation of THz waves. The detecting beam was focused onto a GaAs crystal for the detection of the THz wave by electro-optic sampling. Two polyethylene lenses were used to collimate and focus the emitted THz radiation onto the sample. The transmitted THz wave was collected and focused onto the GaAs crystal with two polyethylene lenses. The detectable spectral range was from 0.7 to 1.6 THz (23–53 cm^{-1}) with a sensitivity of signal to noise (S/N) of 1000 in the electric field amplitude. The time resolution for the THz measurement was 66.6 fs, and the spot size was 5 mm in diameter. The polarization of the THz beam was perpendicular to the optical axis of the crystal. An all-solid-state green laser (centre wavelength 532 nm) was employed in the experiment to provide an external optical field. The light was obliquely incident upon the surface of the samples at an angle of 45° with respect to the polar axis, and the spot size was 8 mm in diameter. To make sure that the sample was restored to its previous dynamic behaviour, we performed a thermal process after each measurement. The sample was placed in a furnace at 220 °C for 3 h, and no external field was applied to it during this recovery process.

3. Results and discussion

The time domain waveforms were obtained in the experiment as shown in Fig. 2. The time lags between the reference (air) and the two samples were about 2.5 and 2.8 ps, respectively, which can be deduced from Fig. 2(a). The second and third waveforms for the two crystals (dashed line corresponding to near-SLN:Fe, and solid line corresponding to near-SLN:Ce) were introduced by multiple internal reflections of the samples. By applying an external optical field, a time shift could be observed in the time domain. For example, compared to those without light excitation, the transmission waveform of near-SLN:Fe shifted about 0.05 ps when the light intensity was 200 mW/cm^2, and the transmission waveform of near-SLN:Ce shifted about 0.025 ps when the light intensity was 300 mW/cm^2, as shown in Fig. 2(b) and (c), respectively.

Through a Fourier transform, we got the transmission spectra and the intrinsic phase shifts of the samples. The complex refractive index $N^*(f)$ and the permittivity $\varepsilon^*(f)$ were calculated from the THz transmission spectra. Figure 3(a) shows the frequency dependence of the real part of dielectric constant $\varepsilon'(f)$ and its variation under different external optical fields of near-SLN:Fe. The oscillation in the low frequency region was caused by the influence of noise and the absorption of vapour. In the frequency range of 0.7–1.6 THz, the dielectric constant of near-SLN:Fe was about 42–46. The measured permittivity was found to be tunable up to 3% via the application of the external optical field. When the light intensity was lower than 120 mW/cm^2, the dielectric constant nonlinearly decreased with the increase in the green laser power. When the light intensity was around 160 mW/cm^2, the dielectric constant increased suddenly, and then decreased again with the increase in light power.

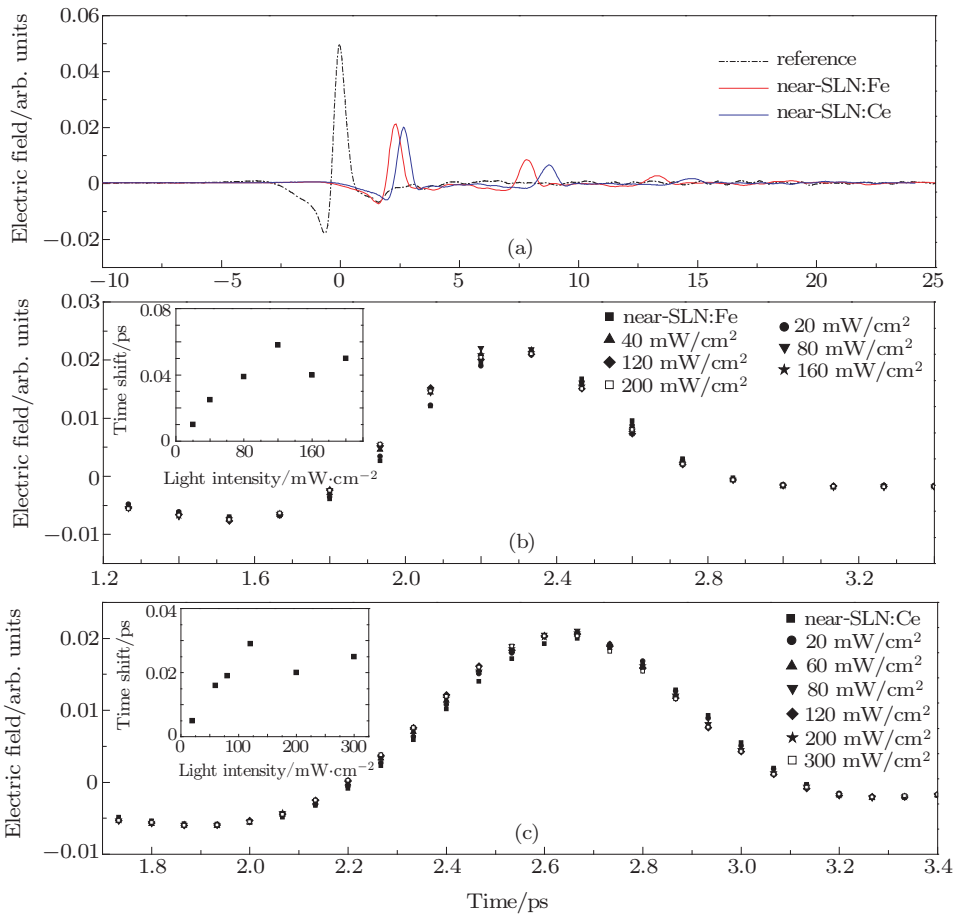


Fig. 2. (a) (colour online) Time domain transmission waveforms of near-SLN:Fe and near-SLN:Ce crystals. Panels (b) and (c) show the time shifts of near-SLN:Fe and near-SLN:Ce under different external optical fields at room temperature, respectively. The inserts show the time shifts (relative to the curve of zero intensity) as functions of the applied intensity.

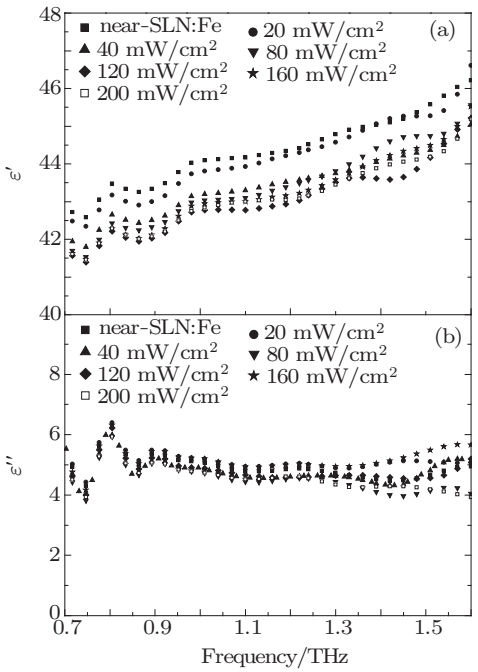


Fig. 3. Frequency dependence of (a) the real part and (b) the imaginary part of the complex dielectric constant of the near-SLN:Fe crystal with different external optical fields at room temperature.

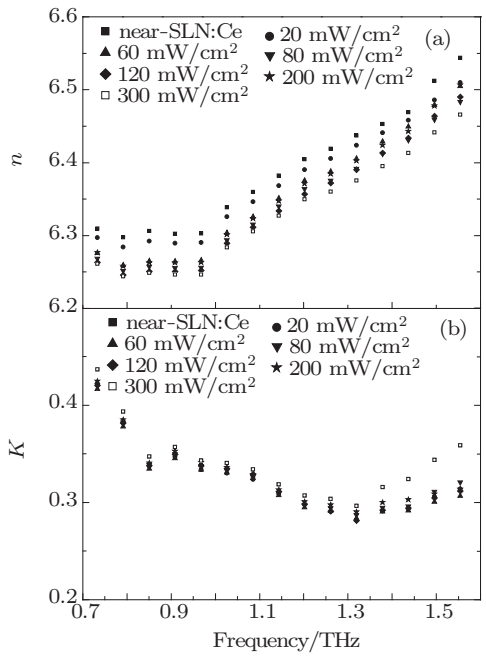


Fig. 4. Frequency dependence of (a) the real part and (b) the imaginary part of the complex refractive index of the near-SLN:Ce crystal with different external optical fields at room temperature.

Figure 4(a) shows the frequency dependence of the real part of refractive index $n(f)$ and its variation under different external optical fields of near-SLN:Ce. In the frequency range of 0.7–1.6 THz, the refractive index of near-SLN:Ce was about 6.3–6.6 (corresponding to the permittivity of 39–43). When the light intensity was lower than 120 mW/cm^2, the refractive index decreased with the increase in green laser power. When the light intensity was around 200 mW/cm^2, the refractive index increased suddenly and then decreased again with the increase in light power.

In contrast, Figs. 3(b) and 4(b) demonstrate that the imaginary parts of the dielectric constants of both near-SLN:Fe and near-SLN:Ce crystals under different external optical fields do not show obvious differences, indicating that the dielectric loss does not change appreciably with the increase in the external optical field. This may be attributed to the fact that two loss mechanisms are responsible for the dielectric loss under the external field: a conduction loss $\tan\delta_{\rm R}$ and an intrinsic loss $\tan\delta_{\rm C}$.[18,19] The intrinsic loss factor is reduced when the external optical field is applied, while the conduction loss increases with the increase in the optical field strength. Since the influence of the optical field on the loss of the specimens is minor, as shown in Figs. 3(b) and 4(b), this indicates that the effect of the intrinsic loss counteracts that of the conduction loss.

In order to illustrate the microscopic process in the crystals clearly, it is worth studying the variation of their refractive indexes. Figure 5 shows the modulation of the refractive index of near-SLN:Fe as a function of the applied light intensity and its fitting. When the light intensity was less than 120 mW/cm^2, the variation of refractive index, $|\Delta n|$, was found to be proportional to the intensity of the applied light. The results can be described by using a relationship proposed by Chen[20]

$$\Delta n = \frac{1}{2}(n_{\rm o}^3\gamma_{13} - n_{\rm e}^3\gamma_{33})E_3 \propto I, \qquad (1)$$

where $n_{\rm o}$ and $n_{\rm e}$ are the refractive indexes of the ordinary and the extraordinary lights, respectively, γ_{ij} is the linear optoelectronic coefficient, E_3 is the internal space charge field along the polar axis, and I is the applied light intensity. This result indicates that the change in the refractive index dispersion of near-SLN:Fe may be attributed to the internal space charge field in the crystal caused by the space displacement of the excited free carriers.

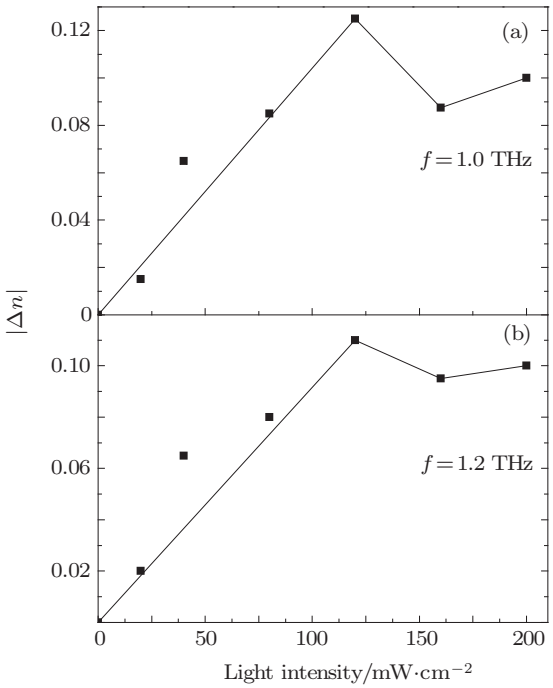


Fig. 5. The light intensity dependence of the variation in refractive index of near-SLN:Fe at (a) 1.0 THz and (b) 1.2 THz. The squares are our measured values, and the solid lines are the fittings.

When the light intensity was 160 mW/cm^2, the variation of refractive index, $|\Delta n|$, showed a step-like decrease. For example, at a frequency of 1.0 THz, $|\Delta n|$ decreased to 0.08 at a light intensity of 160 mW/cm^2, and then increased sightly again with increasing light intensity. This phenomenon was introduced by the light-induced domain reversal in the crystal.

For the near-SLN:Ce crystal, we can obtain a similar phenomenon. The photorefraction, $|\Delta n|$, had a linear relationship with the intensity of the applied light when the intensity was less than 120 mW/cm^2, and then showed a step-like decrease at a light intensity of 200 mW/cm^2, as shown in Fig. 6. The light intensity, at which the step-like decrease in the photorefraction took place in near-SLN:Ce, was a little higher than that in the near-SLN:Fe crystal. This difference is related to the micro structures of the two crystals. Moreover, the variation in refractive index of near-SLN:Ce was less than that of near-SLN:Fe. For example, $|\Delta n|$ could reach 0.12 in near-SLN:Fe, while it could only get to about 0.05 in the near-SLN:Ce crystal.

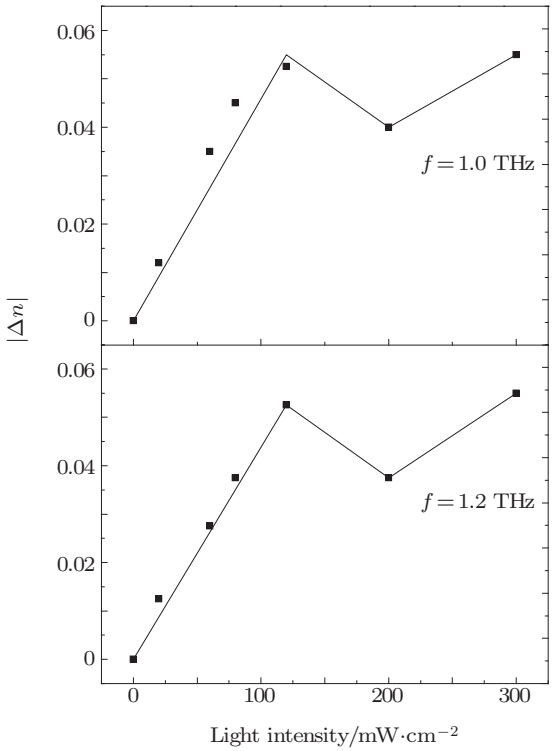


Fig. 6. Light intensity dependence of the variation in refractive index of near-SLN:Ce at (a) 1.0 THz and (b) 1.2 THz. The squares are our measured values, and the solid lines are the fittings.

The micro mechanisms behind the observed effects are discussed as follows. (i) Both Fe^{2+} and Fe^{3+} ions in near-SLN:Fe crystals are octahedrally coordinated by six oxygen atoms and occupy the Li^{1+} sites,[21] while Ce^{3+} and Ce^{4+} ions in near-SLN:Ce occupy the antisite Nb^{5+}, which results in lots of free electrons in near-SLN:Fe and lots of holes in near-SLN:Ce. When the external optical field is applied, the free electrons and the free holes migrate in preferred directions. The dominant charge driving force is the photovoltaic effect. Drift and diffusion could also have contributions to the movement of the electrons and the holes. The thermal excitations are negligible here. Then the space displacements of the carriers lead to an internal space charge field shielding the macroscopic spontaneous polarization of the crystals. The internal field causes a variation in the refractive index via the linear electro-optic effect.[20] As we know, the mobility of electrons is much larger than that of holes. So the internal space charge field in near-SLN:Fe is larger than that in near-SLN:Ce under the the same applied light, resulting in a more obvious photorefractive effect in near-SLN:Fe than that in near-SLN:Ce, as shown in Figs. 5 and 6. (ii) When the light intensity is higher than 120 mW/cm^2, the internal space charge field in near-SLN:Fe (or in near-SLN:Ce) is sufficiently enhanced so that a light-induced domain reversal occurs in the crystal, which results in the electric neutralization of some of the space charge. Another electric field, which is induced by the screening charge on the surface, could have an additional contribution to the domain reversal.[10] Then the domain walls of the reversed domain do not have plenty of negative bound charge, which induces the weakening of the space charge field, leading to the corresponding decrease in photorefraction. The light intensity, at which the step-like decrease in photorefraction takes place in near-SLN:Ce, is a little higher than that in near-SLN:Fe. This means that the coercive field in near-SLN:Ce is slightly larger than that in near-SLN:Fe, which can also be attributed to the photorefraction resistance behaviour of the near-SLN:Ce crystal.

4. Conclusion

In summary, we investigated the frequency dependence of the dielectric spectra of iron-doped and cerium-doped near-stoichiometric lithium niobate crystals at room temperature. The photorefractive effect was demonstrated in both near-SLN:Fe and near-SLN:Ce, with different levels of external optical fields. This property originates from the internal space charge field caused by the free carriers apart from the light-induced domain reversal, which leads to a step-like decrease in the photorefraction in the crystal. We presume that the two mechanisms would complement each other, resulting in the observed photoferroelectric behaviours in near-SLN:Fe and near-SLN:Ce.

References

[1] Gunter P and Huignard P J 1988 1989 *Photorefractive Materials and Their Applications I and II* (Eidelberg: Springer-Verlag)
[2] Banfi G P, Datta P K, Degiorgio V and Fortusini D 1998 *Appl. Phys. Lett.* **73** 136
[3] Bermúdez V, Capmany J, GarcíaSolé J and Diéguez E 1998 *Appl. Phys. Lett.* **73** 593
[4] Pruneri V, Webjörn J, Russell P St J and Hanna D C 1995 *Appl. Phys. Lett.* **67** 2126
[5] Sasaki Y, Yuri A, Kawase K and Ito H 2002 *Appl. Phys. Lett.* **81** 3323
[6] Abernethy J A, Gawith C B E, Eason R W and Smith P G R 2002 *Appl. Phys. Lett.* **81** 2514
[7] Gallo K and Assanto G 2001 *Appl. Phys. Lett.* **79** 314
[8] Zhang Y 2010 *Acta Phys. Sin.* **59** 5528 (in Chinese)
[9] Kahmann F, Pankrath R and Rupp R A 1994 *Opt. Commun.* **107** 6
[10] Wang W J, Kong Y F, Liu H D, Hu Q, Liu S G, Chen S L and Xu J J 2009 *J. Appl. Phys.* **105** 043105

[11] Ling F R, Wang B, Guan C X, Tao G, Teng D D, Yuan W and Sun N 2004 *Opt. Commun.* **241** 293

[12] Wu L, Ling F R, Tian X G, Zhao H T, Liu J S and Yao J Q 2011 *Opt. Mater.* **33** 1737

[13] Jermann F and Otten J 1993 *J. Opt. Soc. Am.* B **10** 2085

[14] Volk T and Wöhlecke M 2008 *Lithium Niobate-Defects, Photorefraction and Ferroelectric* (Berlin: Springer)

[15] Nahata A, Weling A S and Heinz T F 1996 *Appl. Phys. Lett.* **69** 2321

[16] Wu L, Ling F R, Liu T, Liu J S, Xu Y B and Yao J Q 2011 *Opt. Express* **19** 5118

[17] Zhong K, Yao J Q, Xu D G, Zhang H Y and Wang P 2011 *Acta Phy. Sin.* **60** 285 (in Chinese)

[18] Chen Y C, Wu L, Chou Y P and Tsai Y T 2000 *Mater. Sci. Eng.* B **76** 95

[19] Johnson K M 1962 *J. Appl. Phys.* **33** 2826

[20] Chen F S 1969 *J. Appl. Phys.* **40** 3389

[21] Vitova T, Hormes J, Falk Matthias and Karsten B 2009 *J. Appl. Phys.* **105** 013524